Morphotectonic evolution of rifted continental margins: inferences from a coupled tectonic-surface processes model and fission track thermochronology

van der Beek, P.A.; Andriessen, P.A.M.; Cloetingh, S.A.P.L.

published in
Tectonics
1995

DOI (link to publisher)
10.1029/94TC02445

document version
Publisher's PDF, also known as Version of record

TECTONICS, VOL. 14, NO. 2, PAGES 406-421, APRIL 1995

Morphotectonic evolution of rifted continental margins: Inferences from a coupled tectonic-surface processes model and fission track thermochronology

Peter van der Beek, Paul Andriessen, and Sierd Cloetingh

Faculty of Earth Sciences, Vrije Universiteit, Amsterdam, Netherlands

Abstract. We use a numerical model to study the topographic evolution and erosional history of rifted continental margins. The model combines a kinematic description of lithospheric extension ("tectonic model") with a surface processes model that includes short-range hillslope and long-range fluvial transport. The tectonic model predicts the evolution of the lithospheric temperature and strength (elastic thickness) distribution as well as the tectonic uplift through time. This is input into the surface processes model which calculates the degradation of topography and associated isostatic rebound. Modeled denudation histories across the margin are used to predict apatite fission track age and length patterns. Modeling results indicate that, depending on the adopted parameters, an uplifted rift flank should degrade by erosion within 50-100 m.y., without significant retreat of the topographic elevation maximum. The development of an escarpment system at rifted continental margins is in itself not an indication of tectonic rift flank uplift, but results from the existence of a high elevation interior plateau, erosional base-level lowering as a consequence of rifting and regional isostatic response to erosion of the margin. However, apatite fission track thermochronology reveals that the areas seaward of the escarpment at a number of rifted margins have been exhumed from several kilometers depth. Such amounts of denudation cannot be accommodated with isostatic rebound alone and require additional tectonic uplift of the rift flanks. Modeling of apatite fission track patterns suggests that fission track thermochronology dates the onset of rapid erosion which coincides with the initiation of strong relief (i.e., initiation of rifting). Fission track ages which are younger than the age of rifting thus cannot be unambiguously interpreted as excluding prerift uplift. The timing of margin uplift can be established only by careful track length analysis and integration with regional stratigraphic data. The model is applied to the Saudi Arabian Red Sea margin and the southeastern Australian highlands, where it is constrained by present-day topography and apatite fission track data, as well as seismic and gravity data. For the Saudi Arabian Red Sea margin, synrift regional plateau uplift with a magnitude of approximately 1 km is inferred, possibly as a result of asthenospheric upwelling. Flexurally induced tectonic uplift of the rift flank with a magnitude of 2 km is superimposed on this regional uplift. The relatively high elevation of the southeastern Australian highlands, their steep front and the relatively high amounts of erosion suggest that, apart from Mesozoic synrift flexural uplift, Tertiary rejuvenation of topography has occurred, possibly as a result of renewed lithospheric thinning and underplating. The low elevation of the Australian interior would inhibit the evolution of a major escarpment in the absence of such renewed uplift.

Paper number 94TC02445.
0278-7407/95/94TC-02445$10.00

Introduction

Several rifted continental margins throughout the world show a conspicuous escarpment which separates a high elevation interior plateau from a strongly dissected and low-lying exterior area seaward of the escarpment (Figure 1) [e.g., *Ollier*, 1985]. These escarpment systems offer the possibility to study the interplay between tectonics, erosion and isostatic rebound in shaping topography [e.g., *Stephenson and Lambeck*, 1985; *Gilchrist and Summerfield*, 1990]. The exact mechanism of their formation remains, however, controversial. Escarpments at rifted margins have generally been interpreted in terms of tectonic rift margin uplift as a result of thermal [e.g., *Beaumont et al.*, 1982; *Steckler*, 1985], dynamic [*Turcotte and Emerman*, 1983; *Bois*, 1993; *Ziegler*, 1994], underplating [*McKenzie*, 1984; *White and McKenzie*, 1989] or flexural [*Braun and Beaumont*, 1989; *Weissel and Karner*, 1989, *Kooi et al.*, 1992] forces. The long-lived nature of a number of elevated margins, e.g., those bordering former Gondwanaland, has been used as an argument to rule out thermal or dynamic effects as the major force driving uplift because the thermal time constant of the lithosphere (~60 m.y.) is too small to support rift shoulders existing since the Mesozoic [*Weissel and Karner*, 1989]. For mechanisms resulting in permanent uplift (e.g., flexure and underplating) the life span of a rift shoulder should be controlled by an erosional time constant. Such a quantity is, however, poorly understood and may vary strongly according to nontectonic factors such as climate and lithology. A number of authors [e.g., *Gilchrist and Summerfield*, 1990; *Brown*, 1991; *Gallagher et al.*, 1994] have pointed out that escarpment systems flanking rifted margins are primarily maintained by a high-elevation interior plateau and regional isostatic response to denudation as a result of base level lowering during rifting. Therefore regional plateau uplift (acting on a subcontinental scale) might be the main tectonic mechanism responsible for the existence of escarpments, with rift flank uplift (affecting only the margin itself) playing a secondary role.

Another question regards the timing of the main uplift phase with respect to rifting [e.g., *Garfunkel*, 1988; *Bohan-*

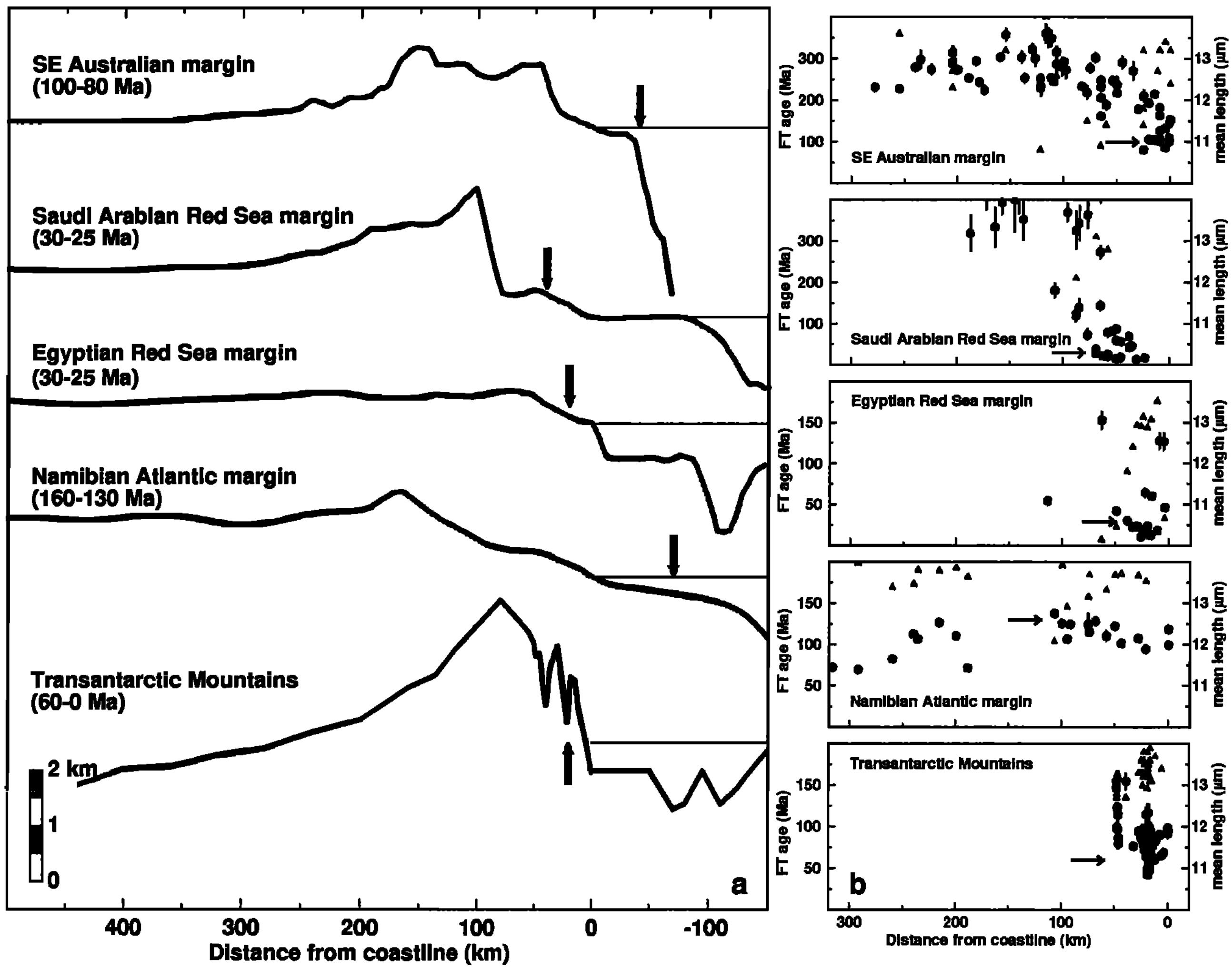

Figure 1. (a) Topographic profiles of selected rifted continental margins showing the characteristic morphology of an escarpment separating an elevated interior plateau from a low-lying exterior area, as well as the morphological variations between margins. The profiles are aligned at the coastline, arrows indicate the approximate location of the master fault bounding the rifted basin; the distance between this and the top of the escarpment represents the amount of erosional retreat. Numbers in parentheses indicate timing of rift phase. (b) Patterns of apatite fission track (FT) ages (dots with error bars) and mean track lengths (open triangles) across these margins. Arrows denote timing of initiation of rifting. Data are from *Moore et al.* [1986] and *Dumitru et al.* [1991] for southeastern Australia, *Bohannon et al.* [1989] for Saudi Arabia, *Omar et al.* [1989] for Egypt, *Brown et al.* [1990] for Namibia, and *Gleadow and Fitzgerald* [1987] and *Fitzgerald* [1992] for the Transantarctic Mountains.

non et al., 1989; *Omar et al.*, 1989]. This has important implications for geodynamic models of rift initiation and evolution. Whereas "active" rifting models, involving mantle plume activity, predict regional plateau uplift preceding the main rifting phase by some 30-60 m.y. [*White and McKenzie*, 1989], "passive" models predict rift flank uplift coinciding with extension [e.g. *Steckler*, 1985; *Braun and Beaumont*, 1989]. Recently, a number of authors have suggested that regional uplift may also postdate the main rifting phase by 10-20 m.y. [*Menzies et al.*, 1992; *Bois*, 1993; *Ziegler*, 1994], suggesting a change in rift mode from "passive" to "active" during the evolution of the rift.

The erosional development of elevated rifted margins is slowly becoming better understood. A widely held view [e.g., *Ollier*, 1985; *Weissel*, 1990; *Summerfield*, 1991; *Tucker and Slingerland*, 1994] is that the characteristic concave morphology of escarpment systems evolves by parallel erosional retreat. Erosion rates are highest along the edge of the escarpment because of high relief. Intermediate erosion rates are recorded in the exterior areas where fluvial systems carry the debris of escarpment erosion away. Inland of the escarpment, erosion rates, with transport of material toward the hinterland, are generally low.

During recent years, apatite fission track thermochronology has received increased attention as a means of establishing a record of rift margin uplift, analogous to the stratigraphy of the sedimentary infill which records basin subsidence. The continuous production and subsequent annealing of fission tracks registers the low-temperature (< 120°C) cooling path of a sample as annealing rates increase from extremely slow at surface temperatures to virtually instantaneous (< 1 m.y.) at ~120°C. Samples exhumed from different depths (paleotemperatures) will therefore have different fission track ages and track length distributions [e.g., *Gleadow and Fitzgerald*, 1987]. Recent advances in the understanding of the kinetics of apatite fission track annealing [e.g., *Green et al.*, 1989] have made it possible to quantitatively resolve cooling paths from fission track data [cf. *Lutz and Omar*, 1991]. Thus apatite fission track thermochronology can be used to constrain the erosional history of a region, if the geothermal gradient is sufficiently well known [e.g., *Brown et al.*, 1994].

Several fission track studies [e.g., *Moore et al.*, 1986; *Bohannon et al.*, 1989, *Gallagher et al.*, 1994] have revealed a typical pattern of fission track ages and track length distributions at rifted continental margins (Figure 1b). Samples from close to the basin edge typically have fission track ages younger than the age of rifting and relatively high mean track lengths, indicating that they experienced temperatures > 120°C prior to rifting. Fission track ages usually increase rapidly over the escarpment, while mean lengths first decrease and subsequently increase away from the coastline, indicative of samples exhumed from subsequently lower temperature ranges (Figure 2). The observed patterns suggest that rocks exposed in the area seaward of the escarpment have been exhumed from depths of 3-4 km since the onset of rifting. These studies thus support the conceptual models of escarpment evolution and suggest a "passive" origin for rift margin uplift.

By backstacking the inferred amount of eroded material onto the present-day topography the tectonic and isostatic components of uplift can be resolved [e.g., *Brown*, 1991]. Using this method we have shown [*van der Beek et al.*, 1994] that for reasonable estimates of lithospheric strength, significant tectonic rift flank uplift (of the order of 3-5 km) must have taken place at a number of continental margins. Forward tectonic modeling supports a flexural origin for this uplift.

In this paper, we focus on the temporal evolution of rifted continental margins. *Kooi and Beaumont* [1994] used a surface processes model developed by *Beaumont et al.* [1992] to study the controls on escarpment evolution; the insights derived from this work were used by *Gilchrist et al.* [1994] to study the denudation history of southwestern Africa. Here, we aim to combine this surface processes model with tectonic uplift patterns predicted by a forward model of rifted margin evolution [*Kooi et al.*, 1992] in order to predict the morphologic evolution and erosional history of rifted continental margins (Figure 3). From the exhumation history we calculate fission track age and length distribution patterns across the margins and compare our predictions with present-day topography and fission track data.

We begin with an outline of the tectonic and surface processes models, followed by modeling experiments carried out to obtain insight into how the interplay between tectonic uplift, erosion, and isostatic rebound affect the evolution of

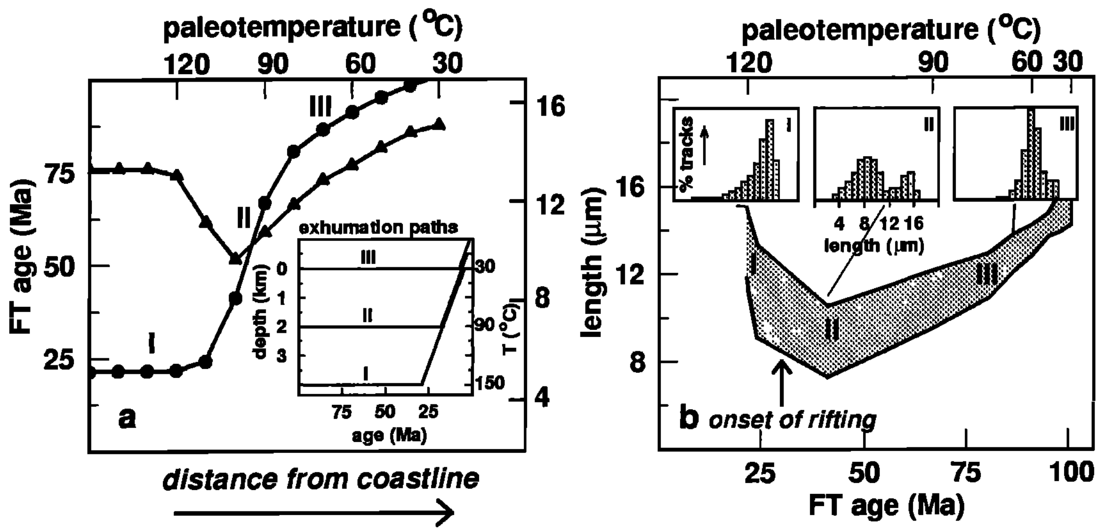

Figure 2. Conceptual model interpreting fission track (FT) age patterns across escarpments at rifted continental margins. (a) Pattern of fission track ages (dots) and mean track lengths (triangles) expected when samples from closest to the shoreline were exhumed from greatest depths (paleotemperatures). Inset shows simplified exhumation paths of samples from the close to the shoreline (I), the base (II), and the top (III) of the escarpment, for a model of exhumation by escarpment retreat. Fission track parameters were calculated using the quantitative annealing model of *Laslett et al.* [1987]. (b) Resulting age-length plot; shaded area represents mean length ± standard deviation for samples from different paleotemperatures (scale on top). Insets show modeled fission track length distributions for samples having experienced the exhumation paths (I, II and III) depicted in Figure 2a. Model is after *van der Beek et al.* [1994].

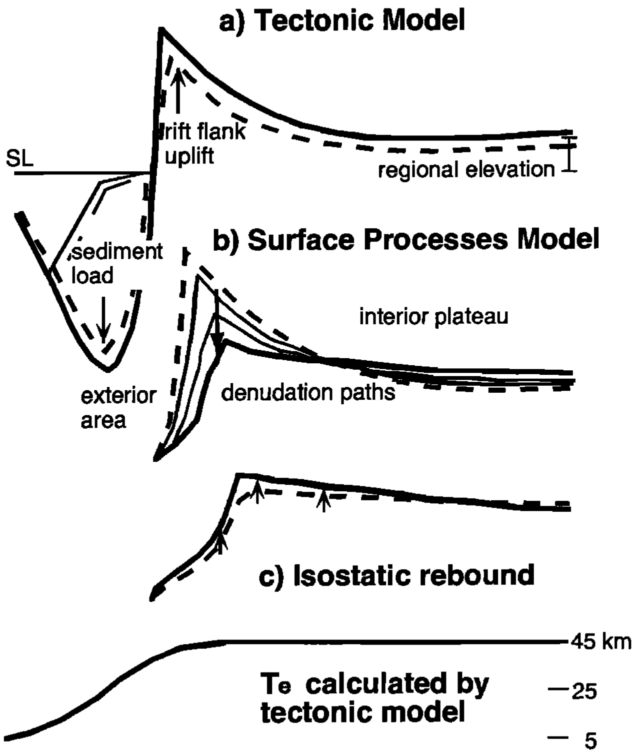

Figure 3. Cartoon of modeling approach showing the coupling between tectonic and surface processes models and the modeling sequence through successive time-steps. (a) The lithospheric extension model calculates tectonic uplift; (b) the surface processes model calculates the degradation of topography, the denudation history is tracked for points across the margin; (c) isostatic rebound is calculated adopting a temporally and spatially varying elastic thickness (T_e) predicted by the tectonic model.

the margin and the observed fission track age/length patterns. We concentrate on two questions: (1) the relative importance of regional elevation (plateau uplift) versus rift flank uplift and (2) the timing of uplift with respect to rifting. We will then present two case studies, the Saudi Arabian Red Sea margin and the southeastern highlands of Australia, to quantify how much of the uplift history and mechanisms can be resolved using this approach. The models are constrained by present-day topography and published fission track data, as well as by seismic and gravity data of the crustal structure underlying the margins. The insights we gain from such a model should contribute to the understanding of the dynamics of rift flank uplift and also have implications for models of paleo-topography and climate evolution [e.g., *Behrendt and Cooper*, 1991].

Modeling Approach

Tectonic Model

The tectonic model of continental rifting we employ is based on the concept of lithospheric "necking" [*Braun and Beaumont*, 1989] and proceeds from a kinematic formulation of lithospheric extension around a reference or "necking" level [*Kooi et al.*, 1992]. During rifting a kinematic surface depression $S_{(x)}$ is induced that is controlled by the depth z_c of this level and the amount of extension β:

$$S_{(x)} = \left(1 - \frac{1}{\beta_{(x)}}\right) z_c \qquad (1)$$

The thermal evolution of the stretched lithosphere is tracked by a finite difference algorithm; vertical motions are calculated by regionally distributing all forces acting on the lithosphere (i.e., thermal forces, forces arising from the kinematic displacements of density interfaces and from erosion and sedimentation) assuming that the elastic thickness of the lithosphere is controlled by the depth to a specified isotherm (here 400°C). Therefore the lithosphere retains finite strength during rifting. The dynamic interpretation of such a model has been discussed extensively by, among others, *Kooi et al.* [1992] and *van der Beek et al.* [1994] and is outside the scope of the present paper. The model is able to incorporate finite rifting times and depth-dependent stretching factors. Rift margin uplift can thus be generated in two ways: when z_c is sufficiently deep, a basin develops that is deeper than the isostatically compensated depth and flexural rift flank uplift is induced; when subcrustal stretching factors larger than crustal ones are adopted, thermally supported uplift is generated. The predicted tectonic uplift and lithospheric strength through time are input into the surface processes model (Figure 3). Note that the "tectonic" uplift evolution of the flank in this case includes the effects of thermal subsidence and sediment loading within the adjacent basin, i.e., it is the topography the flank would attain in the absence of erosion.

Surface Processes Model

Dynamic erosion/sedimentation models rely on developing a relationship between topography $h(x)$ and erosion rate (dh/dt) [e.g., *Leeder*, 1991; *Summerfield*, 1991]. Here, we use a general model developed by *Beaumont et al.* [1992] and *Kooi and Beaumont* [1994] that combines short-range hillslope transport with long-range fluvial transport. Simple linear diffusion models have been used in studies of stratigraphic basin development [e.g., *Kenyon and Turcotte*, 1985; *Flemings and Jordan*, 1989; *van Balen and Cloetingh*, 1994] as well as for modeling the erosion of fault scarps [e.g., *Hanks et al.*, 1984] and tilted fault blocks [*Waltham*, 1992]. However, whereas linear diffusion laws are adequate to simulate either subaerial or submarine slope processes, they fail to predict the characteristic behavior of an escarpment system: preservation of topographic roughness and parallel retreat [*Newman and Turcotte*, 1990; *Weissel*, 1990]. Fluvial transport needs to be incorporated when studying morphologic evolution on this scale [*Kirkby*, 1971]. Specifically, it is the interplay between rates of sediment supply by weathering and transport by hillslope and fluvial processes which determines the resulting morphology of the margin [*Kooi and Beaumont*, 1994; *Tucker and Slingerland*, 1994].

The model proceeds from combining the one-dimensional continuity equation:

$$\frac{dh}{dt} = -\frac{\delta q}{\delta x} \qquad (2)$$

with a sediment transport law q [*Kirkby*, 1971]. Hillslope transport is modeled as a diffusive process [*Culling*, 1960; *Carson and Kirkby*, 1972] with a transport law q_s:

$$q_s = -\kappa \frac{\delta h}{\delta x} \qquad (3)$$

where κ is a linear transportation coefficient with units of square meters per year. Long-range fluvial transport is based on the carrying capacity q_f^{eqb} of river systems transporting sediment away from the escarpment:

$$q_f^{eqb} = -K_f \, q_{r(x)} \frac{\delta h}{\delta x} \qquad (4)$$

This expression includes a discharge term q_r which is a function of the distance from the drainage divide (the escarpment) and a (dimensionless) long-range fluvial transport coefficient K_f. The actual river transport q_f is connected to the equilibrium carrying capacity through a term called the "length scale" of erosion/sedimentation by *Beaumont et al.* [1992]:

$$\frac{\delta q_f}{\delta x} = \frac{1}{l_f}\left(q_f^{eqb} - q_f\right) \qquad (5)$$

Note that the length scale l_f controls the rate at which the disequilibrium of the system tends to be reduced; l_f can take different values for erosion (l_e) or sedimentation (l_s).

The modeling procedure involves determining, for each time step, the position of the drainage divide x_d, $(dh/dx)_x$, and $(d^2h/dx^2)_x$ using backward differences for the slopes. The transport fluxes q_s and q_f, and resulting $(dh/dt)_x$ are subsequently tracked from the escarpment downward to the left and right sides of the model. The spatial step size is 10 km in all models; time steps are adapted to keep the explicit finite difference scheme stable and are of the order of 500 to 1000 years. The model is one-dimensional and we assume that $q_{r(x)}$ increases linearly away from the escarpment: $q_{r(x)} = v_r|x - x_d|$, where v_r is a constant precipitation rate (in meters per year). We interpret the resulting profile to be the along-strike average of topography. As boundary conditions we take $(dh/dt)_0 = 0$ and $(dh/dt)_{xmax} = 0$ so that both sides of the model act as sediment sinks.

The surface processes model does not include deposition of sediments into the offshore basin. Instead, subsidence induced by sedimentation is calculated by the tectonic model, adopting a sediment fill up to a given water depth profile (Figure 3a). We have chosen for this procedure to have a better control on sediment loading; if only the material eroded from the seaward side of the escarpment were deposited into the basin, we would end up with a strongly underfilled basin because sediment supply by river systems breaching the escarpment, along-axis transport, and non-clastic sedimentation are ignored [cf. *van Balen and Cloetingh*, 1994]. Topography is updated by incremental tectonic uplift and isostatic response to erosion every 1-5 m.y. (Figure 3c). When updating the topography for uplift and isostatic rebound, the shoreline ($x = 0$) is kept fixed, the right side of the model ($x = x_{max}$) is free to move.

The evolution of the escarpment system is strongly

Table 1. Modeling Parameters Employed in This Study

Parameter	General models	Red Sea	SE Australia
Tectonic model			
Lithospheric thickness L, km	150	200	150
Crustal thickness c, km	35	40	40
Maximum elastic thickness T_e, km (400°C isotherm)	45	60	45
Necking depth z_c, km	5-15-25	15	20
Surface processes model			
Short-range diffusion coefficient κ, $m^2\,yr^{-1}$	3	5	2
Long-range fluvial transport coefficient × precipitation $K_f v_r$, m y^{-1}	0.01	0.01	0.004
Length scale for fluvial erosion l_e, km	20	20	20
Length scale for fluvial deposition l_s, km	1	1	1

dependent on the adopted values for the surface process parameters κ, K_f, and l_f [cf. *Kooi and Beaumont*, 1994]. Their relative magnitudes determine the morphology of the escarpment system, whereas their absolute magnitudes determine erosion rates. The control of these parameters on the escarpment evolution and their interpretation in terms of climatic and lithological factors was elaborated upon by *Kooi and Beaumont* [1994] and *Gilchrist et al.* [1994] and is beyond the scope of this paper. We will use average values that lead to reasonable erosion/retreat rates (Table 1), representing escarpment development under supply-limited ("arid") conditions [cf. *Kooi and Beaumont*, 1994; *Tucker and Slingerland*, 1994]. This implies that our model is strictly valid only for constant climatic conditions and uniform bedrock.

Calculating Fission Track Parameters

The surface processes model predicts the final topography as well as exhumation (depth-time) paths for each point across the margin. From these we can calculate the trend of fission track ages and track length distributions across the escarpment (Figure 2) for a specified relationship between depth and temperature (geothermal gradient) and between temperature and the rate of fission track annealing.

In the following models we adopt a constant geothermal gradient of 30°C/km. The assumption of a constant geotherm in the upper few kilometers of the margin implies that thermal effects of rifting and erosion are minor there. Our tectonic model predicts relatively constant heat flow through time adjacent to a (pure shear) rifted margin, with a less than 10% increase immediately adjacent to the basin as a result of lateral heat flow. Predicted exhumation rates are sufficiently slow (of the order of 10-100 m/m.y.) for isotherms in the upper crust not to be significantly perturbed [cf. *Stüwe et al.*, 1994].

We adopt the kinetic model of *Laslett et al.* [1987] to predict fission track ages and length distributions from the model temperature-time paths [cf. *Green et al.*, 1989; *Lutz and Omar*, 1991]. Fission tracks are produced with a standard length (16 μm) at a constant rate throughout the modeled time span. Once a track is produced, its subsequent annealing (track length reduction r) is followed through successive time steps:

$$\{[(1-r_j^{\,b})/b]^a - 1\}/a \;=\; T_j\{C_0 + [C_1 \ln(t_{eq} + \Delta t_j) + C_2]\} \tag{6}$$

where T_j and Δt_j are the temperature during and duration of the jth time-step, respectively, a, b, C_0, C_1 and C_2 are constants [*Laslett et al.*, 1987], and t_{eq} is the "equivalent time" representing the total amount of annealing at the onset of the j^{th} time-step [*Duddy et al.*, 1988]. Fission track age is calculated from the set of differentially annealed tracks using a linear relationship between track density and track length [*Lutz and Omar*, 1991]. The set of reduced track lengths is transformed into a binned fission track length distribution histogram by integrating a Gaussian probability density function over the length bins [*Lutz and Omar*, 1991]. In order to have a better comparison between calculated and observed fission track length distribution we introduce the postulated observational bias toward longer mean track lengths [*Laslett et al.*, 1982] in the binning.

Controls on Margin Evolution

In the following we assess the importance of the different components of tectonic uplift, erosion, and isostatic rebound in creating topography at elevated rifted margins. We investigate how the relative contributions of regional plateau uplift and flexural rift flank uplift affect the morphologic evolution and fission track patterns of a model rifted margin. Subsequently, we discuss the effects of a different timing of regional uplift with respect to rifting on the resulting topographic evolution and erosion patterns.

Figure 4 illustrates the effect of varying regional elevation (caused by prerift plateau uplift) and synrift flank uplift. Modeled rift flank uplift is flexural in nature; different amounts of uplift are created by varying the kinematic level of "necking". Figure 4 shows the topographic evolution of the margin, the total amount of uplift, erosion, and isostatic rebound, and predicted fission track patterns across the escarpment 50 m.y. after rifting.

Figure 4a illustrates the evolution of a high rift flank, supported by a deep level of necking (25 km), and a low-lying interior area. Because of high topographic gradients inland of the rift flank, erosion toward the hinterland is very effective. The more or less symmetrical gradients inhibit hinterward retreat of the escarpment, which remains at the locus of maximum tectonic uplift (see also *Kooi and Beaumont* [1994]). The rift flank degrades within 50 to 100 m.y., depending on the adopted constants in the erosion model. Maximum erosion, amounting to more than 3 km, takes place just behind the locus of maximum tectonic uplift, leading to young fission track ages close to the basin. From ~100 km landward, net sedimentation occurs in what can be called a "hinterland basin" [*Ten Brink and Stern*, 1992].

In contrast, Figure 4b shows the evolution of an escarpment along a high elevated plateau. The regional elevation of the interior plateau is 1000 m, and very little additional flank uplift takes place during rifting, as a result of shallow necking (5 km). In this case erosion takes place seaward of the escarpment, and escarpment retreat is initiated virtually instantly after rifting. Retreat rates start out relatively fast and slow down during the postrift evolution. Maximum erosion is less than 2 km. The elevation of the escarpment increases as it retreats, as a result of increasing isostatic response to erosion. Because of the relatively small amount of erosion seaward of the escarpment, no rocks have been exhumed from temperature ranges >90°C. As a consequence, fission track ages across the margin are much older than the age of rifting.

Finally, Figure 4c displays a model that includes both an elevated plateau and rift flank uplift. This model leads to maximum erosion of the exterior area and the development of an escarpment system. Escarpment retreat can commence only when the initial rift flank has eroded away; after that, the tectonic uplift pattern is not reflected in the topography. Predicted fission track ages and track length distributions across the escarpment agree well with those generally observed: rocks exposed in the exterior area have been exhumed from depths >3 km and have fission track ages younger than the initiation of uplift, with high mean track lengths; ages increase rapidly toward the escarpment; samples with intermediate ages have lowest mean lengths.

The behavior observed in Figure 4 suggests that the existence of an escarpment along a rifted continental margin

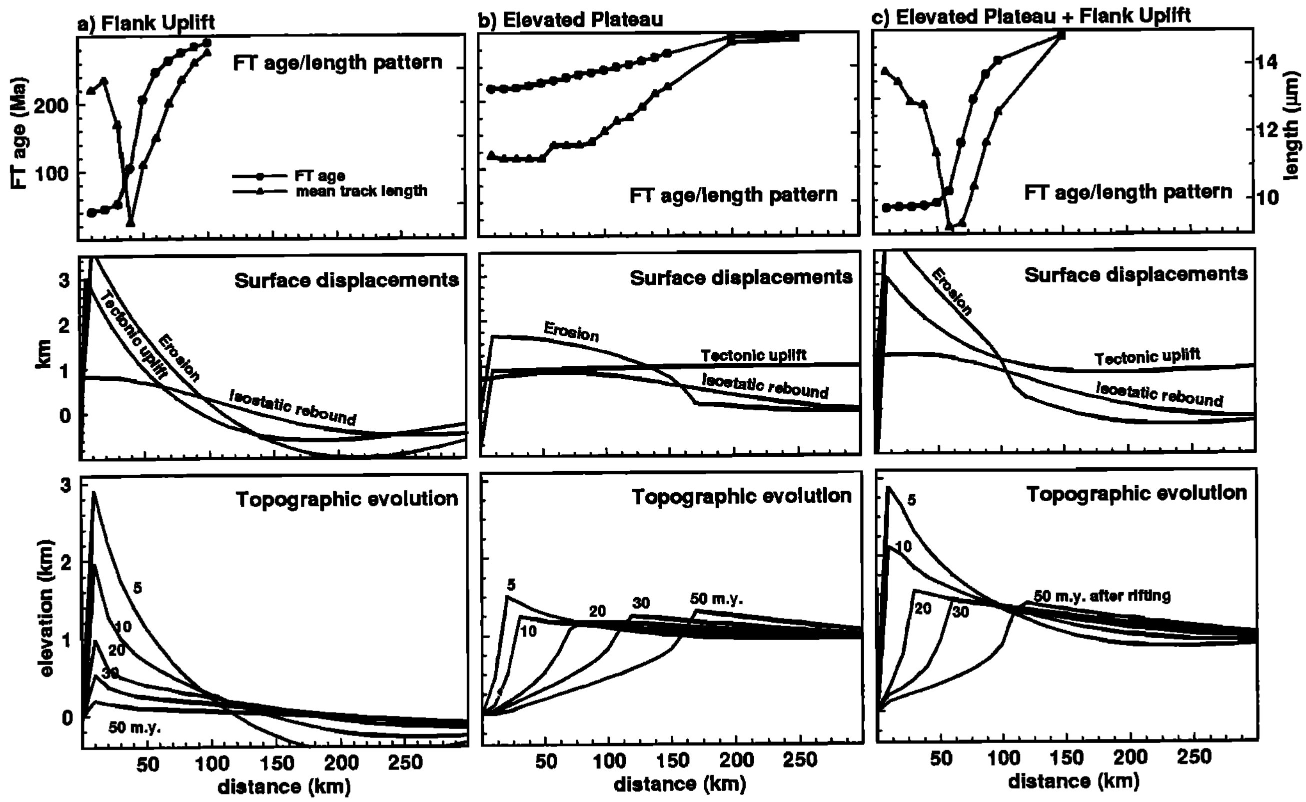

Figure 4. Model rift flank evolution (lower panels), contributions to surface displacement (middle panel), and fission track (FT) age/length patterns (upper panel) 50 m.y. after rifting, for different amounts of rift flank uplift and regional plateau uplift. Modeling parameters are given in Table 1. (a) Interior area is at sea-level, 3- km-high rift flank is supported by lithospheric necking around a 25-km-deep level; (b) interior plateau with a regional elevation of 1 km; no additional tectonic uplift of rift flank (necking depth of 5 km); (c) interior plateau with elevation of 1 km; tectonic uplift (2 km) of rift flank is induced by 15-km necking depth.

is in itself not an indication of rift flank uplift. Uplifted escarpments are maintained by a high-elevation interior plateau and erosion of the exterior area (see also *Tucker and Slingerland* [1994]); flank uplift alone does not lead to development of an escarpment system. However, the several kilometers of erosion of the exterior area that are recorded by fission track data from a number of rifted margins [e.g., *Moore et al.*, 1986; *Bohannon et al.*, 1989] require that additional rift flank uplift has taken place. This is illustrated in Figure 5, which shows the dependence of model results on the adopted strength of the lithosphere (expressed in terms of the equivalent elastic thickness T_e). Models in Figure 4 have T_e varying between 15 and 45 km. For reasonable strength values ($T_e \geq 15$ km) and a model of rifting of an elevated plateau, the elevation of the escarpment (~1.3 × initial elevation) and maximum amount of erosion (~2 × initial elevation) are not very sensitive to T_e. These numbers slowly increase with increasing retreat of the escarpment and associated widening of the exterior area [*Gilchrist et al.*, 1994]. Large amounts (> 3 km) of erosion without additional rift flank uplift therefore require either extreme escarpment retreat (> 300 km), very high initial elevation of the interior plateau (> 1.5 km), or extremely low T_e values (< 5 km). Low T_e values, however, inhibit the development of the characteristic margin morphology as a result of strong local rebound; moreover, they are not in keeping with strength estimates from coherence analyses nor with the crustal structure observed at rifted margins [cf. *van der Beek et al.*, 1994].

We now turn to the issue of the timing of uplift with respect to rifting. Figure 6 shows predicted topographic evolution, erosion, and fission track patterns for prerift, synrift, and postrift regional uplift. Uplift is generated in this case by excess mantle thinning (subcrustal stretching factors are twice as large as crustal stretching factors) over a 400-km-wide area, in order to simulate the effect of active mantle upwelling. Mantle thinning simultaneously reduces the strength of the lithosphere. Because the regional uplift is thermal in nature, it will relax with time. Prerift uplift is assumed to be initiated 30 m.y. before rifting (at 50 Ma), postrift uplift 30 m.y. after it. Additionally, there is ~1 km of flexural rift flank uplift during rifting. The results indicate that it is very difficult to detect prerift uplift phases from fission track data alone. Even for extreme prerift thermal uplift values (~2 km), prerift erosion is less than 1 km and takes place mainly inland of the present-day escarpment. Erosion patterns and topographic evolution are very similar for prerift and synrift regional uplift; the resulting patterns of fission track ages across the escarpment are therefore also nearly indistinguishable (Figures 6d and 6e). Both models

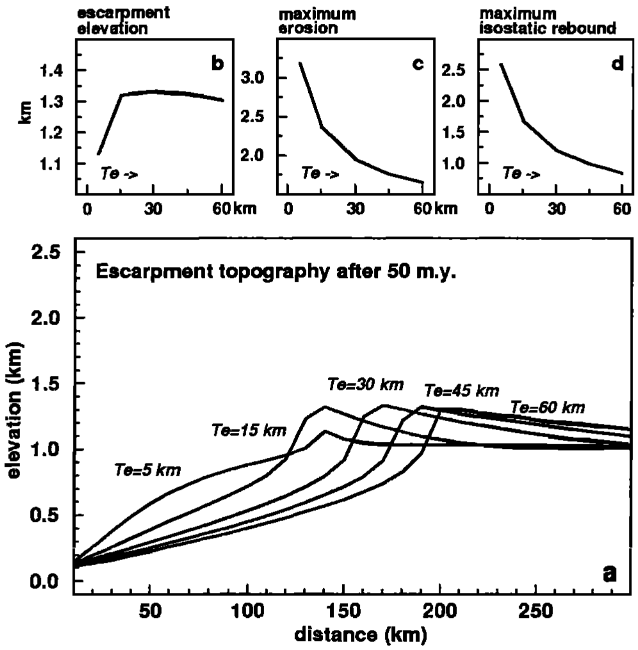

Figure 5. Topographic and erosional development for the model of Figure 4b (interior plateau with 1 km elevation; no additional rift flank uplift) for different constant flexural rigidity (elastic thickness T_e) of the lithosphere. (a) Escarpment morphology 50 m.y. after rifting; note that for very low strength (T_e < 15 km), creation of the characteristic concave morphology is inhibited by large local rebound. (b) Maximum escarpment height, (c) maximum erosion, and (d) maximum isostatic rebound 50 m.y. after rifting, as a function of T_e.

predict fission track ages which are younger than the age of rifting seaward of the escarpment. Postrift uplift shows a contrasting evolution with far less erosion taking place and the development of a high and steep escarpment, because erosion rates cannot keep up with recent tectonic uplift. The timing of initiation of uplift can be inferred from plots of fission track age against mean track length [e.g., *Omar et al.*, 1989]. Here, there is a slight difference between the predictions of the prerift and synrift regional uplift models; mean track lengths increase at older fission track ages for the prerift model (Figure 6e) as a result of (slow) prerift exhumation/cooling. The young age peak in these plots, however, dates the onset of rapid rift-related erosion in all three cases.

Modeling Regional Examples

In the following, we use our model to study the evolution of two "real-world" examples: the Saudi Arabian Red Sea margin and the southeastern Australian highlands. For both of these margins a suitable database exists, with onshore and offshore seismic and gravity data constraining the structure of the margin, and extensive fission track control on the exhumation history. In this exercise we concentrate on two questions, regarding the problems posed in the previous section: (1) can we determine the timing of margin uplift with respect to rifting and (2) can we quantify the relative magnitude of rift flank uplift compared to regional plateau uplift? Of course, in modeling the complex morphotectonic evolution of an actual rifted margin, simplifying assumptions are inevitable. For instance, possible thermal effects of rifting are incorporated in a crude way and we do not consider possible changes in erosional parameters as a result of climate or lithology. Nevertheless, the first order characteristics of the evolution of these margins seem to be reproduced by the model.

Saudi Arabian Red Sea Margin

Rifting in the central and southern Red Sea started approximately 30 m.y. ago, lasted for about 5 m.y. and led to continental breakup at 25 Ma [*Bohannon*, 1986]. The Saudi Arabian Red Sea margin is characterized by a prominent escarpment which is located 100-150 km inland from the shoreline; the escarpment peaks rise up to 1500-2000 m, while the interior Arabian platform lies at an elevation of around 1000 m. Major normal faults bounding the highly extended Red Sea basement are encountered up to 40 km inland [*Bohannon*, 1986]; the escarpment thus retreated approximately 100 km.

Apatite fission track ages for the Saudi Arabian Red Sea margin decrease from ~400 Ma inland of the escarpment to < 30 Ma near the shoreline [*Bohannon et al.*, 1989], providing evidence for 3-4 km of erosion seaward of the escarpment since the onset of rifting. Flexural backstacking of the inferred amount of erosion shows that the margin must have experienced more than 3 km of tectonic uplift [*van der Beek et al.*, 1994]. Rift flank uplift is, however, superimposed on much more widespread plateau uplift which causes the high elevation of the Arabian platform. Late Eocene-Oligocene shallow marine sediments occur on the Arabian platform [*Garfunkel*, 1988; *Bohannon et al.*, 1989], indicating that this uplift occurred simultaneously with or postdated rifting. *Camp and Roobol* [1992] and *Menzies et al.* [1992] suggest that regional uplift is the result of active mantle upwelling beneath the Arabian subcontinent which may have commenced as late as 15 m.y. ago. In the northern Red Sea, conglomerates dated at 16-17 Ma seem to indicate increased uplift and erosion around that time [*Garfunkel*, 1988]. However, *Steckler and Omar* [1994] provide evidence for an onset of uplift at least 21 m.y. ago.

We model the erosional and topographic evolution of the margin using a tectonic model of pure-shear stretching, incorporating regional plateau uplift and flexural rift flank uplift induced by lithospheric necking around a midcrustal (15 km) level. This model provides the best fit to the present-day topography and total (backstacked) tectonic uplift, as well as to gravity and seismic data [*van der Beek et al.*, 1994]. Assuming an initial lithospheric thickness of 200 km (a reasonable value considering the late Proterozoic age of the Arabian lithosphere) and T_e defined by the 400°C isotherm leads to a lithospheric strength evolution with T_e diminishing from 60 km in the interior platform to approximately 25 km adjacent to the Red Sea basin.

Figure 7 shows the evolution of topography, tectonic uplift, erosion, and predicted fission track age patterns for a model in which all regional uplift is synrifting, i.e., occurs between 30 and 25 Ma. This leads to a high (~2.5 km) rift flank at the end of rifting, which degrades in approximately

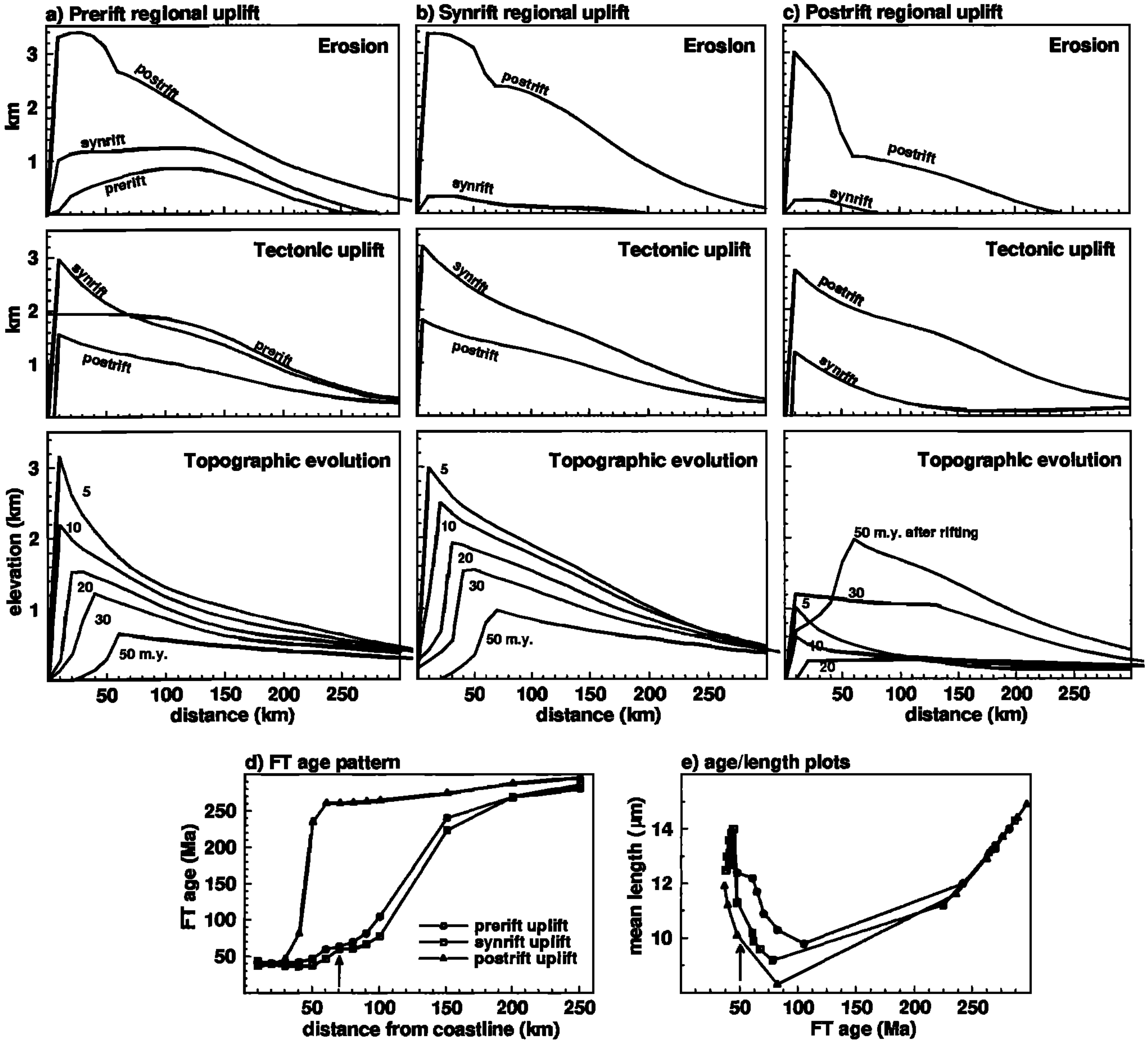

Figure 6. Model rift flank evolution for regional plateau uplift as a resulting of excess lithospheric thinning; (a) predating rifting by 30 m.y., (b) occurring simultaneous with rifting at 50 Ma, and (c) postdating rifting by 30 m.y.. Lower panels show postrift evolution of rift flank morphology, middle panels prerift, synrift, and postrift contributions to tectonic uplift, and upper panels prerift, synrift, and postrift erosion of the margin. (d) Pattern of fission track (FT) ages across the escarpment 50 m.y. after rifting; vertical arrow denotes position of escarpment. (e) Corresponding age/length plots; arrow denotes timing of initiation of rifting.

10 m.y. and then starts retreating, adopting the parameters from Table 1. Predicted present-day topography and fission track age patterns are in agreement with observed values. Fission track length distributions were reported for five samples only [*Bohannon et al.*, 1989]. Predicted mean track lengths seaward of the escarpment are about 1 µm lower than those observed, while on the interior plateau they are about 1 µm higher.

Alternative tectonic scenarios are depicted in Figure 8; Figure 8a shows the topographic evolution and calculated fission track ages for a model of linear regional plateau uplift from 30 Ma onward and Figure 8b for a model in which regional uplift only commences after 15 Ma. Rift flank uplift is similar, both in timing (30-25 Ma) and amount (~2 km), to the first model. These models predict much less impressive topography during rifting. The flexurally supported rift flank reaches an elevation of approximately 1 km; while it degrades, the interior plateau is uplifted and an escarpment starts to develop. Because regional uplift occurs later in these models, a higher elevation of the area seaward of the

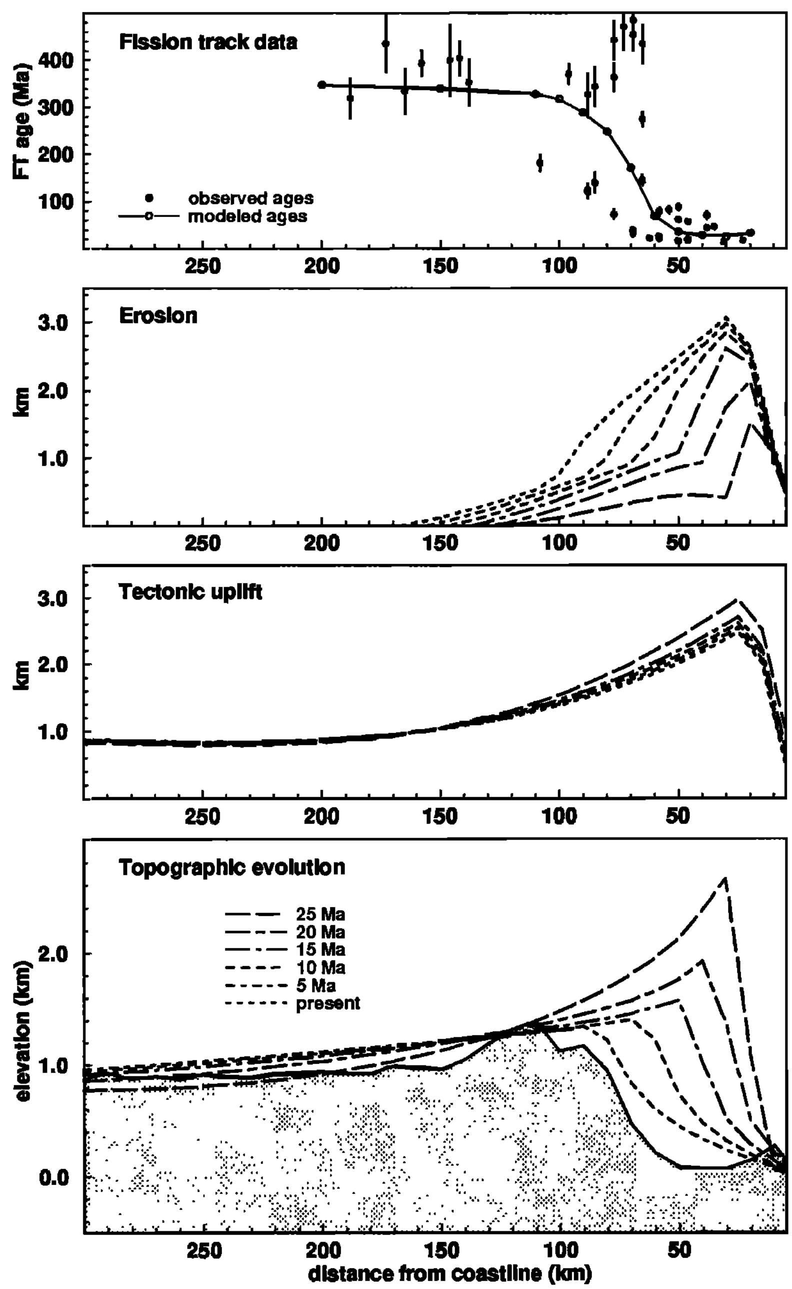

Figure 7. Modeled topographic evolution, tectonic uplift, and erosion through time and predicted fission track (FT) ages for the Saudi Arabian Red Sea margin, for a model with a 200 km thick lithosphere, 2-km flexural uplift of rift flank, and 1 km regional plateau uplift from 30 to 25 Ma. Shaded area in lower panel indicates observed present-day topography. The group of high fission track ages near 70 km are samples from significantly higher elevations than the modeled profile.

escarpment and less erosion are predicted. It is difficult to discriminate between a model of synrift and continuous postrift regional uplift; both models produce erosion patterns which fit the fission track data within error. Models in which most regional uplift occurs late, in contrast, predict too little erosion of the exterior area for constant erosion/retreat rates. Young (< 20 Ma) fission track ages which were encountered in some samples from the Saudi Arabian and Yemenese margins have been cited as indicating relatively young uplift [e.g., *Menzies et al.*, 1992]. However, care should be taken in directly relating the exhumation recorded by fission track data into tectonic uplift. The modeling presented here suggests that, if anything, younger uplift leads to older fission track ages seaward of the escarpment. Of course, the assumption underlying this conclusion is that the parameters controlling erosion rates have been constant throughout the evolution of the margin, i.e., no climate change has taken place and a homogeneous bedrock has been eroded. The

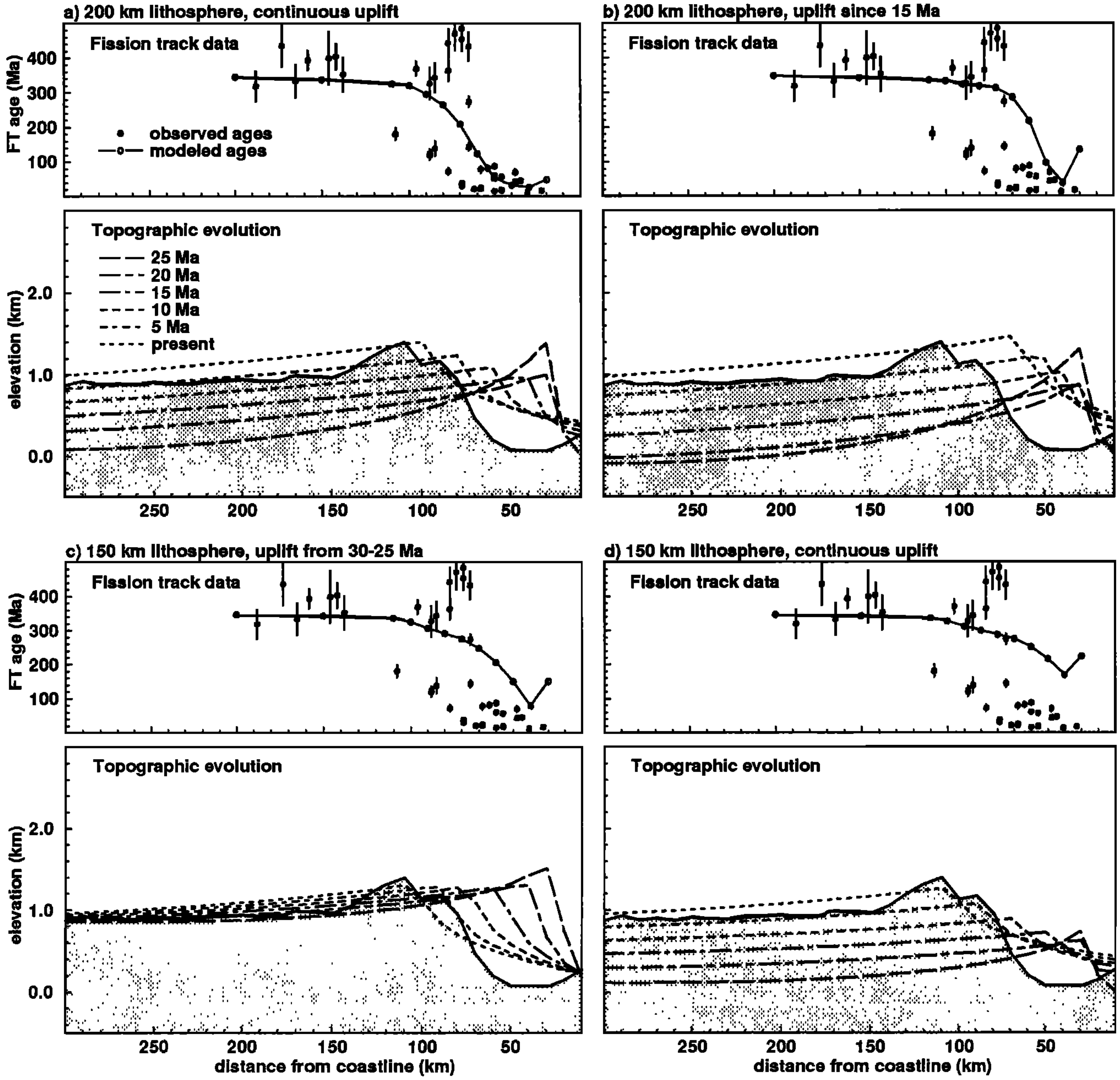

Figure 8. Modeled topographic evolution and predicted fission track (FT) ages for different uplift scenarios for the Saudi Arabian Red Sea margin: (a) 200-km lithosphere, 2-km flexural uplift of rift flank from 30 to 25 Ma, and 1-km regional plateau uplift from 30 Ma onward to present day; (b) same as Figure 8a but with regional uplift starting at 15 Ma; (c) 150-km lithosphere, leads to much less (500 m) tectonic uplift of rift flank and more isostatic rebound, 1-km regional uplift from 30 to 25 Ma; (d) same as Figre 8c but with regional uplift from 30 Ma onward.

latter assumption is demonstrably not valid at the Red Sea margins, as erosion has stripped away both a Phanerozoic sedimentary cover and parts of the crystalline basement [*Garfunkel*, 1988; *Steckler and Omar*, 1994] which presumably have a lower erodibility.

The model has been rerun adopting a lithospheric thickness of 150 km and an associated maximum T_e = 45 km. This leads to significantly less flexural flank uplift (~ 500 m) and more isostatic rebound as a response to erosion. As discussed in the previous section, a model without significant rift flank uplift leads to less erosion seaward of the escarpment (e.g., Figure 4). In the case of the Saudi Arabian Red Sea margin, such a model fails to explain the fission track data which record 3-4 km of erosion (Figures 8c and 8d).

Southeastern Australian Highlands

The southeastern Australian highlands extend along the continental margin of eastern Australia, with the highest peaks located approximately 100-150 km from the coastline. Maximum elevation is over 1500 m, while the Australian interior lies at an altitude below 200 m. The timing of uplift of the southeastern Australian highlands has been a subject of debate for decades, with estimates for the initiation of uplift varying between the Paleozoic and Late Tertiary [e.g., *Veevers*, 1984; *Lambeck and Stephenson*, 1986; *Wellman*, 1987]. The highlands expose rocks of the Paleozoic Lachlan fold belt, which record extensive compressional deformation and widespread magmatism [e.g., *Fergusson and Coney*, 1992], presumably associated with the generation of high elevation and relief. Late Paleozoic-Mesozoic clastic sediments occur in the basins surrounding the southeastern highlands, indicating that they were a source of sediments, and thus a topographic high, during this time [e.g., *Lambeck and Stephenson*, 1986].

Moore et al. [1986] and *Dumitru et al.* [1991], however, present apatite fission track data that indicate a thermal pulse between 100 and 80 Ma and significant (~2-3 km) erosion since then. Heating of the margin is suggested by strongly bimodal track length distributions in samples with intermediate ages, erosion by samples with young ages (≤ 80 Ma) and high mean lengths. The inferred timing immediately precedes continental breakup in the Tasman Sea (79-72 Ma), supporting a model in which the highlands were uplifted during rifting, with subsequent erosional retreat taking place [*Ollier*, 1982; *Veevers*, 1984]. *Veevers* [1984] and *Wellman* [1987] suggested that accelerated uplift and erosion may have occurred during the Cenozoic, coinciding with basaltic volcanism within the range.

We have developed a model of lithospheric extension for the southeastern Australian margin in order to test these suggestions and to evaluate whether this approach can discriminate between them. The tectonic model we employ (parameters are given in Table 1) is designed to provide a fit to the observed depth to basement offshore and to the gravity anomaly pattern. Synrift flank uplift is predicted from a model of flexural support as a result of a deep (20 km) level of "necking". *Etheridge et al.* [1989] suggested a thermal support for the southeastern highlands uplift as a result of simple shear extension. It may be difficult to differentiate between these mechanisms since rifting took place relatively long ago. Heating of the margin, as suggested by fission track length distributions [*Moore et al.*, 1986; *Dumitru et al.*, 1991], is more easily explained by a simple shear model. However, a thermal support would lead to postrift subsidence of the rift shoulders which is not observed [*Wellman*, 1987]. In any case, in a simple shear model incorporating lithospheric strength, flexural flank uplift would dominate thermal effects [e.g., *van der Beek et al.*, 1994]. We calculate the thermal evolution, lithospheric strength, and uplift patterns for Mesozoic (100-80 Ma) rifting only as well as for Mesozoic rifting combined with renewed Cenozoic (20-0 Ma) uplift, starting with a flat topography at 100 Ma.

Figure 9 shows the modeled topographic evolution, tectonic uplift, erosion, and fission track patterns. Fission track parameters were calculated as before, but we employ an elevated geothermal gradient (40°C/km instead of 30°C/km) during rifting, as suggested by *Moore et al.* [1986] and *Dumitru et al.* [1991]. The model with only Mesozoic (100-80 Ma) uplift predicts that very little topography should be left at present. Because of the low elevation of the Australian interior, it is implausible that a high escarpment will develop. Note that the retreat rate in this case must be much lower than for the Saudi Arabian margin (about a factor 2.5). Maximum erosion is about 2 km; as a result, rocks exposed in the exterior area would have experienced peak temperatures not higher than 100°C during rifting. This is reflected in predicted fission track ages that are older than those observed seaward of the escarpment and in mean track lengths that increase monotonically inland from the coastline.

Therefore the present-day high elevation of the southeastern Australian highlands, combined with the erosion rates inferred from the fission track data, seems to suggest that they have been rejuvenated relatively recently. Modeling of the present-day stress field of the Indo-Australian region [*Cloetingh and Wortel*, 1986] suggests that whereas western Australia is presently under compression, eastern Australia should experience tension. *Cloetingh et al.* [1992] inferred from the stratigraphy of the northwestern Australian margin that the present state of stress may have prevailed since 15 Ma. Therefore we believe that Tertiary uplift of the southeastern Australian margin could be a result of renewed lithospheric extension combined with crustal underplating. A model with renewed uplift from 20 Ma onward (modeled by thinning the lithosphere but not the crust; Figure 9b) reproduces the present-day topography as well as the amounts of erosion inferred from the fission track data better. The topographic misfit that both models predict could indicate that, at the onset of rifting, there was residual topography from the Paleozoic orogenies that occurred in the southeastern Highlands, and that the assumption of low prerift elevation is incorrect. However, models which explain the topographic evolution of southeast Australia solely as a result of Paleozoic orogeny, with subsequent erosion and isostatic rebound [e.g., *Lambeck and Stephenson*, 1986] adopt erosion rates which are an order of magnitude lower than those suggested by the fission track data (see also *Brown et al.* [1994]).

Discussion and Conclusions

A critical assumption in the models presented above concerns the rates at which different processes take place. Whereas the rate of tectonic uplift is controlled by the duration of rifting, which can be estimated by studying the field relationships of datable rift-related sediments and magmatic rocks, the rates of surface processes are much more difficult to assess. In the model, erosion rates are controlled by the parameter values κ and $K_f\, v_r$, which are essentially unconstrained. An independent check on (long-term and spatially averaged) erosion rates can be performed by comparing them to results of mass balance studies [e.g., *Garfunkel*, 1988; *Leeder*, 1991] and fission track data. Figure 10 shows modeled tectonic uplift and exhumation paths for the Saudi Arabian and southeast Australian margins, compared to cooling paths which were obtained by inversion of apatite fission track ages and length distributions (see *Lutz and Omar* [1991] for the approach used). Note that modeled exhumation histories, which are generally in agreement with thermal histories obtained from inversion of fission track data, may differ significantly from the tectonic uplift paths

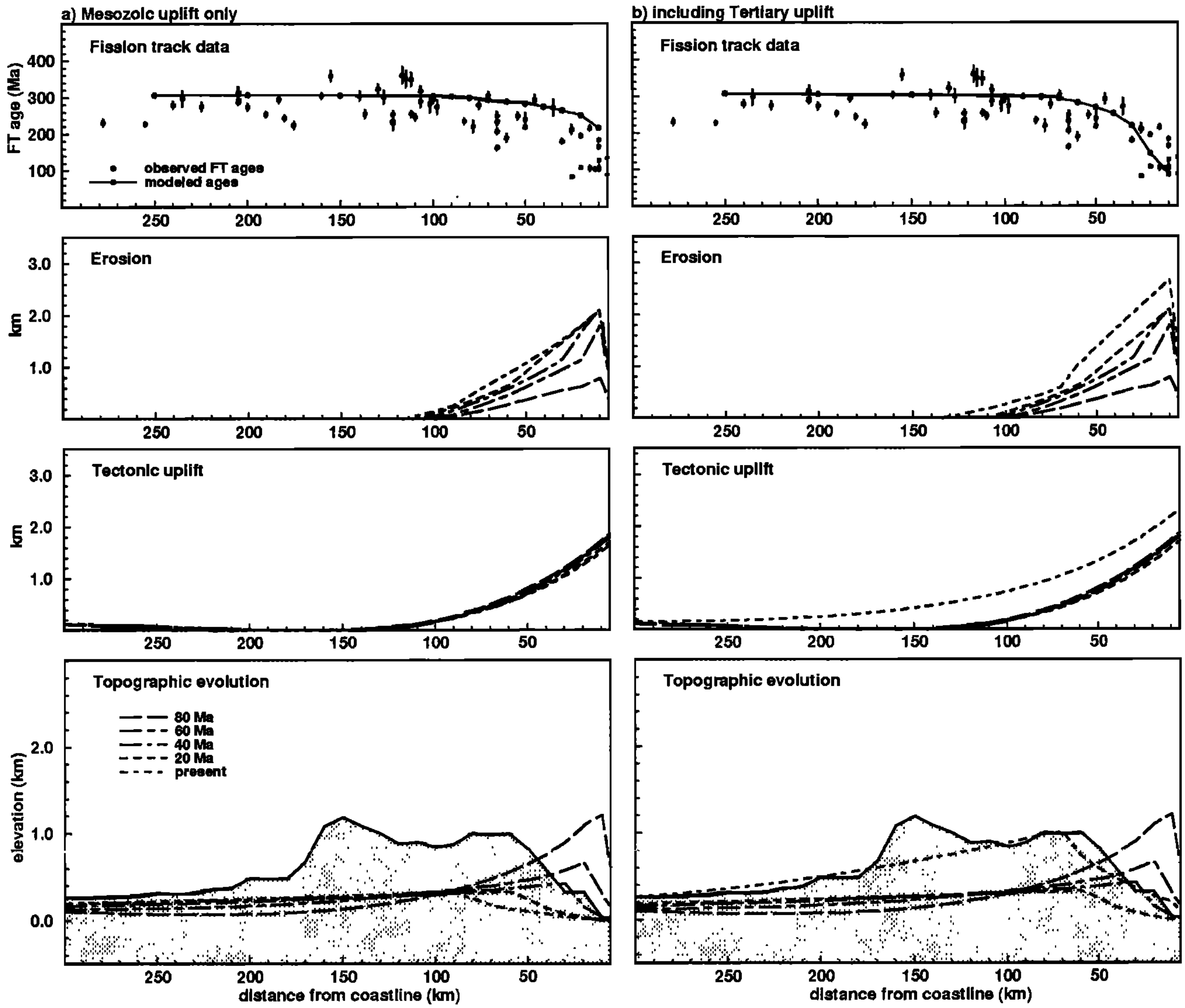

Figure 9. Topographic evolution, tectonic uplift, erosion, and modeled fission track (FT) ages for two models of uplift of the southeastern Australian highlands. (a) Rift flank uplift takes place from 100 to 80 Ma as a result of lithospheric necking; (b) model including rejuvenation of topography by lithospheric thinning and underplating from 20 Ma onward.

that were input into the model. Maximum exhumation rates lag behind maximum tectonic uplift by 5-20 m.y. and occur in the exterior area in the early postrift phase, when the rift flank starts degrading. After the escarpment has retreated away, exhumation rates decrease by a factor of 5-10. Seaward of the escarpment we may therefore discriminate between synrift/early postrift, and postrift erosion, analogous to synrift and postrift sedimentation within the basin. The major difference between the two is that erosion is diachronous across the margin.

Maximum "synrift" exhumation rates from both forward and inverse modeling are 125-225 m/m.y. for the Red Sea and 20-40 m/m.y. for the southeastern Australian highlands. Synrift tectonic uplift rates from forward modeling are in the order of 600 and 100 m/m.y., respectively. Postrift exhumation rates are an order of magnitude lower, at 10-30 m/m.y. for the Saudi Arabian margin and < 10 m/m.y. for southeastern Australia. These values are consistent with rates of synrift uplift and erosion for rifted margins of 50-350 m/m.y. quoted by *Leeder* [1991] and with values of 6-15 m/m.y. given by *Wellman* [1987] for the southeastern Australian highlands. Of course, these values could vary in time as a result of climatic change or varying bedrock lithologies. However, temporal variations in erosion parameters seem exceedingly difficult to detect and can, at present, be dealt with in a speculative manner at best.

The inferred rates of tectonic uplift and erosion suggest that, generally, the topography of a rift flank should grow during rifting until a certain threshold value is attained where erosion can keep up with tectonic uplift. Parameter values which lead to reasonable erosion rates predict that such a threshold value is reached only for very high relief. Continu-

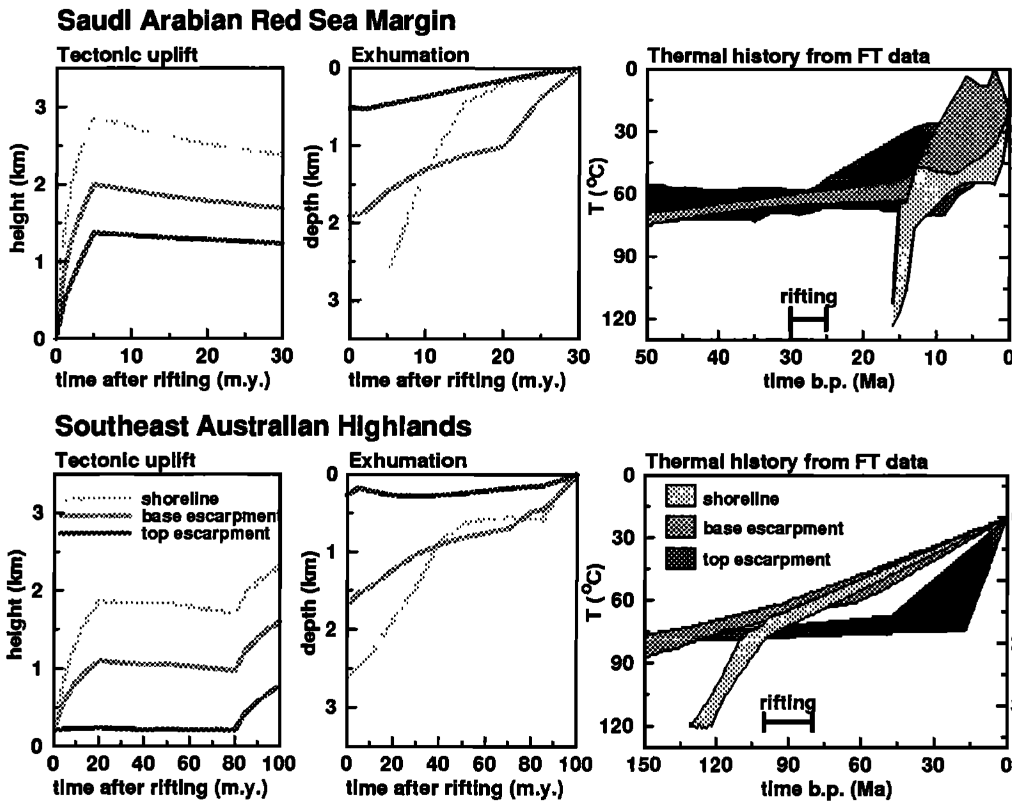

Figure 10. Comparison of modeled tectonic uplift and erosion rates with cooling/exhumation paths from inversion of fission track (FT) data for the Saudi Arabian Red Sea margin and southeastern Australian highlands. Modeled tectonic uplift and exhumation histories are calculated from the preferred models (compare Figures 7 and 9b). Thermal histories were calculated for representative samples from *Bohannon et al.* [1989] for Saudi Arabia and *Moore et al.* [1986] for southeastern Australia. Note different timescales between upper and lower figures. Inversion of fission track age and length distribution was done using the Monte Carlo approach of *Lutz and Omar* [1991] and the annealing model of *Laslett et al.* [1987].

ous uplift of the area immediately adjacent to the basin, as predicted by most models of rift flank uplift, inhibits the evolution of an effective fluvial transport system toward the basin. It is during the early postrift phase that the most rapid degradation of the rift flank takes place and a retreating escarpment system can start to develop. The Transantarctic Mountains, which transect the Antarctic continent from the Ross to the Weddell seas, could be an example of an actively uplifting rift flank system. They present the most impressive rift flank topography on Earth (Figure 1), while their highest summits are located only ~50 km inland of the locus of maximum uplift [*Fitzgerald*, 1992]. There are numerous arguments in favor of continuous extension in the Ross Sea (at varying rates) since its onset approximately 60 m.y. ago [*Behrendt and Cooper*, 1991; *Fitzgerald*, 1992]. Because of continuous tectonic uplift, with denudation lagging behind, the elevation of the mountain range has probably grown continuously since the onset of rifting.

We have shown that the development of an escarpment system is mainly controlled by the elevation of the interior plateau and that the pattern of tectonic uplift is generally not reflected in the escarpment topography (Figure 4). Therefore an interpretation of long-lived escarpments along, for instance, the Mesozoic margins of Gondwanaland as tectonically supported rift flanks is too simple. A tectonic uplift component within elevated escarpments can be detected by backstacking the amount of erosion that has taken place seaward of the escarpment [*van der Beek et al.*, 1994]. Rift flanks which are supported by permanent uplift mechanisms (e.g., flexure) should also degrade, by hinterlandward erosion, within 50-100 m.y.. This may have happened at the eastern margin of North America where Early Cretaceous sediments overstepped the paleorift flank 60-65 m.y. after Early-Middle Jurassic rifting in the North Atlantic [*Steckler et al.*, 1988]. Late Jurassic-Early Cretaceous fission track ages (~140-150 Ma [*Miller and Duddy*, 1989; *Steckler et al.*, 1993]) along the margin support such a hypothesis. The Egyptian margin of the Red Sea seems to be presently in a such a state of degradation. It is conspicuously lower than the Arabian margin (Figure 1a), and the morphology of the margin suggests significant erosion and transport toward the Nile river system in the hinterland (J. K. Weissel, personal communication, 1992). The marked differences between the eastern and western margins of the Red Sea seem therefore to be mainly the result of the elevation difference of the Egyptian and Arabian interior plateaus and the consequent effectiveness of material transport toward the hinterland.

The strong variation in morphology between different elevated rifted margins (Figure 1) thus seems to be the result of varying amounts of rift flank uplift and regional elevation.

At one end of the spectrum (regional elevation has strongest control on the margin morphology) could be, for instance, the southern African and southeast Brazilian Atlantic margins [*Brown et al.*, 1990; *Gallagher et al.*, 1994]; at the other end (topography is mainly controlled by rift flank uplift) could be the Transantarctic Mountains. The Saudi Arabian Red Sea margin would then be an intermediate case where both regional elevation and rift flank uplift play a role. *Ten Brink and Stern* [1992] explained such differences in morphology by different boundary conditions at the margin: a continuous elastic plate would lead to a "southern African" morphology, while a broken plate would result in "Transantarctic Mountain-like" rift flanks. The mechanism proposed here, however, seems to be much more logical and self-consistent. Of course, the high elevation of the interior plateaus of, for instance, Arabia, southern Africa, and Brazil also needs a dynamic explanation. It may result from regional uplift driven by active mantle upwelling initiated sometime during rifting [*Camp and Roobol*, 1992; *Bois*, 1993; *Ziegler*, 1994] and/or crustal underplating associated with flood basalt-type magmatism [*McKenzie*, 1984; *Gallagher et al.*, 1994].

The dynamics of such regional uplift can possibly be inferred from its timing. Prerift, synrift, and postrift regional uplift have each been proposed, for instance, for the Arabian peninsula [e.g., *White and McKenzie*, 1989; *Omar et al.*, 1989; *Menzies et al.*, 1992]. Attempts have been made to constrain the timing of regional uplift from fission track studies. However, as shown in Figures 6 and 10, the interpretation of fission track ages in terms of timing of uplift is not straightforward, because the erosional response acts as a filter between them (see also *Steckler and Omar* [1994]). Basically, fission track data record the onset of rapid erosion which coincides with generation of major relief. Prerift thermal domes may have a high elevation but, because of their long-wavelength nature, have low relief and, consequently, denudation will be slow (up to an order of magnitude slower than for high-relief rift flanks). This is exemplified by the East African dome, the Miocene-Recent uplift of which is not well recorded by fission track data [e.g., *Wagner et al.*, 1992]. Therefore, the best approach to determine the presence or absence of significant prerift uplift remains studying the stratigraphic relationships between prerift and synrift rocks on the margin and analyzing the basin fill [e.g., *Garfunkel*, 1988; *Menzies et al.*, 1992].

The modeling performed here is still prone to significant uncertainties concerning the nature and rate of processes acting on rifted margins, and seriously simplified assumptions. For instance, the assumption of a constant geotherm ignores the thermal perturbations associated with rifting. Although our forward model suggests that these may be minor in the upper few kilometers of the crust adjacent to the basin, fission track data from, for instance, the southeastern Australian highlands seem to suggest some thermal disturbance. Also, we have chosen to adopt constant transport parameters in the surface processes models, implying constant climatic conditions and uniform eroding bedrock. An attempt to get a better handle on these parameters may be most challenging.

Nevertheless, the model seems capable to predict first-order characteristics of rifted margin evolution. For the Saudi Arabian Red Sea margin modeling suggests that regional uplift of the Arabian platform should be accompanied by approximately 2 km of rift flank. Although the timing of plateau uplift cannot be easily resolved, it does not seem plausible that much of it took place very late in the evolution of the rift, while stratigraphic data constrain it to be synrift to postrift. In the case of the southeastern Australian highlands renewed Tertiary uplift has to be invoked to explain the present-day topography and the amounts of erosion recorded seaward of the escarpment.

These examples indicate the potential and necessity of including the tectonic and surface processes acting on a rifted margin and recorded by fission track thermochronology in integrated basin studies, in order to understand the dynamics of rift basin evolution and its sedimentary infill.

Acknowledgments. We thank Henk Kooi for support in developing the model and for numerous suggestions and comments on an earlier version of this paper. Discussions with Randell Stephenson and Ronald van Balen are gratefully acknowledged. This paper benefitted from constructive reviews by Cynthia Ebinger, Kerry Gallagher, and Dale Sawyer. This is Neth. Res. School Sedim. Geol. publication 940801.

References

Beaumont, C., C.E. Keen, and R. Boutillier, On the evolution of rifted continental margins: Comparison of models and observations for the Nova Scotia margin, *Geophys. J. R. Astron. Soc.*, *70*, 667-715, 1982.

Beaumont, C., P. Fullsack, and J. Hamilton, Erosional control of active compressional orogens, in *Thrust Tectonics*, edited by K.R. McClay, pp. 1-18, Chapman and Hall, London, 1992.

Behrendt, J.C., and A. Cooper, Evidence of rapid Cenozoic uplift of the shoulder escarpment of the Cenozoic West Antarctic rift system and a speculation on possible climate forcing, *Geology*, *19*, 315-319, 1991.

Bohannon, R.G., Tectonic configuration of the western Arabian continental margin, southern Red Sea, *Tectonics*, *5*, 477-499, 1986.

Bohannon, R.G., C.W. Naeser, D.L. Schmidt, and R.A. Zimmerman, The timing of uplift, volcanism, and rifting peripheral to the Red Sea: A case for passive rifting?, *J. Geophys. Res.*, *94*, 1683-1701, 1989.

Bois, C., Initiation and evolution of the Oligo-Miocene rift basins of southwestern Europe: Contribution of deep seismic reflection profiling, *Tectonophysics*, *226*, 227-252, 1993.

Braun, J., and C. Beaumont, A physical explanation of the relation between flank uplifts and the breakup unconformity at rifted continental margins, *Geology*, *17*, 760-764, 1989.

Brown, R.W., Backstacking apatite fission track "stratigraphy": A method for resolving the erosional and isostatic rebound components of tectonic uplift histories, *Geology*, *19*, 74-77, 1991.

Brown, R.W., D.J. Rust, M.A. Summerfield, A.J.W. Gleadow, and M.C.J. De Wit, An Early Cretaceous phase of accelerated erosion on the south-western margin of Africa: Evidence from apatite fission track analysis and the offshore sedimentary record, *Nucl. Tracks Radiat. Meas.*, *17*, 339-350, 1990.

Brown, R.W., M.A. Summerfield, and A.J.W. Gleadow, Apatite fission track analysis: Its potential for the estimation of denudation rates and implications for models of long-term landscape development, in *Process Models and Theoretical Geomorphology*, edited by M.J. Kirkby, pp. 24-53, John Wiley, New York, 1994.

Camp, V.E., and M.J. Roobol, Upwelling asthenosphere beneath Western Arabia and its regional implications, *J. Geophys. Res.*, *97*, 15,255-15,271, 1992.

Carson, M.A., and M.J. Kirkby, *Hillslope Form and Process*, 475 pp., Cambridge University Press, New York, 1972.

Cloetingh, S., and R. Wortel, Stress in the Indo-Australian plate, *Tectonophysics*, *132*, 49-67, 1986.

Cloetingh, S., C. Stein, P.H.M. Reemst, F. Gradstein, P. Williamson, N. Exon, and U. von Rad, Continental margin stratigraphy, deformation, and intraplate stresses for the Indo- Australian region, *Proc. Ocean Drill. Program, Sci. Results, 123*, 671-713, 1992.

Culling, W.E.H., Analytical theory of erosion, *J. Geol., 68*, 336-344, 1960.

Duddy, I.R., P.F. Green, and G.M. Laslett, Thermal annealing of fission tracks in apatite, 3, Variable temperature behaviour, *Chem. Geol., 73*, 25-38, 1988.

Dumitru, T.A., K.C. Hill, D.A. Coyle, I.R. Duddy, D.A. Foster, A.J.W. Gleadow, P.F. Green, B.P. Kohn, G.M. Laslett, and A.J. O'Sullivan, Fission track thermochronology: Application to continental rifting of Southeastern Australia, *APEA J., 31*, 131-142, 1991.

Etheridge, M.A., P.A. Symonds, and G.A. Lister, Application of the detachment model to reconstruction of conjugate passive margins, in Extensional tectonics and stratigraphy of the North Atlantic Margins, edited by A.J. Tankard and H.R. Balkwill, *AAPG Mem. 46*, pp. 23-40, 1989.

Fergusson, C.L., and P.J. Coney, Convergence and intraplate deformation in the Lachlan Fold belt of southeastern Australia, *Tectonophysics, 214*, 417-439, 1992.

Fitzgerald, P.G., The Transantarctic Mountains of Southern Victoria Land: The application of apatite fission track analysis to a rift shoulder uplift, *Tectonics, 11*, 634-662, 1992.

Flemings, P.B., and T.E. Jordan, A synthetic stratigraphic model of foreland basin development, *J. Geophys. Res., 94*, 3851-3866, 1989.

Gallagher, K., C.J. Hawkesworth, and M.J.M. Mantovani, The denudation history of the onshore continental margin of SE Brazil inferred from apatite fission track data, *J. Geophys. Res., 99*, 18,117-18,145, 1994.

Garfunkel, Z., Relation between continental rifting and uplifting: Evidence from the Suez rift and northern Red Sea, *Tectonophysics, 150*, 33-49, 1988.

Gilchrist, A.R., and M.A. Summerfield, Differential denudation and flexural isostasy in formation of rifted-margin upwarps, *Nature, 346*, 739-742, 1990.

Gilchrist, A.R., H. Kooi, and C. Beaumont, The post-Gondwana geomorphic evolution of southwestern Africa: Implications for the controls on landscape development from observations and numerical experiments, *J. Geophys. Res., 99*, 12,211-12,228, 1994.

Gleadow, A.J.W., and P.G. Fitzgerald, Uplift history and structure of the Transantarctic Mountains: New evidence from fission track dating of basement apatites in the Dry Valleys area, southern Victoria Land, *Earth Planet. Sci. Lett., 82*, 1-14, 1987.

Green, P.F., I.R. Duddy, G.M. Laslett, K.A. Hegarty, A.J.W. Gleadow, and J.F. Lovering, Thermal annealing of fission tracks in apatite, 4, Quantitative modeling techniques and extension to geological timescales, *Chem. Geol., 79*, 155-182, 1989.

Hanks, T.C., R.C. Bucknam, K.R. Lajoie, and R.E. Wallace, Modification of wave-cut and faulting-controlled landforms, *J. Geophys. Res., 89*, 5771-5790, 1984.

Kenyon, P.M., and D.L. Turcotte, Morphology of a delta prograding by bulk sediment transport, *Geol. Soc. Am. Bull., 96*, 1457-1465, 1985.

Kirkby, M.J., Hillslope process response models based on the continuity equation, *Spec. Publ. Inst. Br. Geogr., 3*, 15-30, 1971.

Kooi, H., and C. Beaumont, Escarpment evolution on high-elevation rifted margins; Insights derived from a surface processes model that combines diffusion, advection, and reaction, *J. Geophys. Res., 99*, 12,191-12,210, 1994.

Kooi, H., J. Burrus, and S. Cloetingh, Lithospheric necking and regional isostasy at extensional basins, 1, Subsidence and gravity modeling with an application to the Gulf of Lions margin (SE France), *J. Geophys. Res., 97*, 17,553-17,571, 1992.

Lambeck, K., and R. Stephenson, The post-Paleozoic uplift history of southeastern Australia, *Aust. J. Earth Sci., 33*, 253-270, 1986.

Laslett, G.M., W.S. Kendall, A.J.W. Gleadow, and I.R. Duddy, Bias in measurement of fission track length distributions, *Nucl. Tracks Radiat. Meas., 6*, 79-85, 1982.

Laslett, G.M., P.F. Green, I.R. Duddy, and A.J.W. Gleadow, Thermal annealing of fission tracks in apatite, 2, A quantitative analysis, *Chem. Geol., 65*, 1-13, 1987.

Leeder, M.R., Denudation, vertical crustal move ments and sedimentary basin infill, *Geol. Rundsch., 80*, 441-458, 1991.

Lutz, T.M., and G.I. Omar, An inverse method of modeling thermal histories from apatite fission track data, *Earth Planet. Sci. Lett., 104*, 181-195, 1991.

McKenzie, D.P., A possible mechanism of epeirogenetic uplift, *Nature, 307*, 616-619, 1984.

Menzies, M.A., J. Baker, D. Bosence, C. Dart, I. Davison, A. Hurford, M. Al'Kadasi, K. Mc. Clay, A. Al'Subbary, and A. Yelland, The timing of magmatism, uplift and crustal extension: preliminary observations from Yemen, in Magmatism and the Causes of Continental Break-up, edited by B.C. Storey, T. Alabaster, and R.J. Pankhurst, *Geol. Soc. Spec. Publ., London, 68*, 293-304, 1992.

Miller, D.S., and I.R. Duddy, Early Cretaceous uplift and erosion of the northern Appalachian Basin, New York, based on apatite fission track analysis, *Earth Planet. Sci. Lett., 93*, 35-49, 1989.

Moore, M.E., A.J.W. Gleadow, and J.F. Lovering, Thermal evolution of rifted continental margins: New evidence from fission tracks in basement apatites from southeastern Australia, *Earth Planet. Sci. Lett., 78*, 255-270, 1986.

Newman, W.I., and D.L. Turcotte, Cascade model for fluvial geomorphology, *Geophys. J. Int., 100*, 433-439, 1990.

Ollier, C.D., The Great Escarpment of eastern Australia: Tectonic and geomorphic significance, *J. Geol. Soc. Aust., 29*, 13-23, 1982.

Ollier, C.D. (Ed.), Morphotectonics of passive continental margins, *Z. Geomorphol. Suppl., 54*, 120 pp., 1985.

Omar, G.I., M.S. Steckler, W.R. Buck, and B.P. Kohn, Fission track analysis of basement apatites at the western margin of the Gulf of Suez rift, Egypt: Evidence for synchroneity of uplift and subsidence, *Earth Planet. Sci. Lett., 94*, 316-328, 1989.

Steckler, M.S., Uplift and extension at the Gulf of Suez: Indications of induced mantle convection, *Nature, 317*, 135-139, 1985.

Steckler, M.S., and G.I. Omar, Controls on erosional retreat of the uplifted rift flanks at the Gulf of Suez and northern Red Sea, *J. Geophys. Res., 99*, 12,159-12,173, 1994.

Steckler, M.S., A.B. Watts, and J.A. Thorne, Subsidence and basin modeling at the U.S. Atlantic passive margin, in *The Geology of North America, vol. I-2, The Atlantic Continental Margin, U.S.*, edited by R.E. Sheridan, and J.A. Grow, 399-416, Geological Society of America, Boulder, Colo., 1988.

Steckler, M.S., G.I. Omar, G.D. Karner, and B.P. Kohn, Pattern of hydrothermal circulation within the Newark basin from fission-track analysis, *Geology, 21*, 735-738, 1993.

Stephenson, R., and K. Lambeck, Erosion-isostatic rebound models for uplift: An application to southeastern Australia, *Geophys. J. R. Astron. Soc., 82*, 31-55, 1985.

Stüwe, K., L. White, and R.W. Brown, The influ ence of eroding topography on steady-state isotherms. Application to fission track analysis, *Earth Planet. Sci. Lett., 124*, 63-74, 1994.

Summerfield, M.A., Sub-aerial denudation of passive margins: Regional elevation versus local relief models, *Earth Planet. Sci. Lett., 102*, 460-469, 1991.

Ten Brink, U., and T. Stern, Rift flank uplifts and hinterland basins: Comparison of the Transantarctic Mountains with the Great Escarpment of southern Africa, *J. Geophys. Res., 97*, 569-585, 1992.

Tucker, G.E., and R.L. Slingerland, Erosional dynamics, flexural isostasy, and long-lived escarpments: A numerical modeling study, *J. Geophys. Res., 99*, 12,229-12,243, 1994.

Turcotte, D.L., and S.H. Emerman, Mechanisms of active and passive rifting, *Tectonophysics, 94*, 39-50, 1983.

van Balen, R.T., and S. Cloetingh, Tectonic control of the sedimentary record and stress-induced fluid flow: constraints from basin modeling, in *Origin, Migration and Evolution of Fluids in Sedimentary Basins*, edited by J. Parnell, *Geol. Soc. Spec. Publ., London, 78*, 9-26, 1994.

van der Beek, P.A., S. Cloetingh, and P. Andries sen, Mechanisms of extensional basin formation and vertical motions at rift flanks: Constraints from tectonic modeling and fission track thermo chronology, *Earth Planet. Sci. Lett., 121*, 317-330, 1994.

Veevers, J.J. (Ed.), *Phanerozoic Earth History of Australia*, Clarendon, Oxford, 1984.

Wagner, M., R. Altherr, and P. Van den haute, Apatite fission-track analysis of Kenyan basement rocks: Constraints on the thermotectonic evolution of the Kenya dome. A reconnaissance study, *Tectonophysics, 204*, 93-110, 1992.

Waltham, D., Mathematical modeling of sedimentary basin processes, *Mar. Petrol. Geol., 9*, 265-273, 1992.

Weissel, J.K., Long-term erosional development of rifted continental margins: Toward a quantitative understanding, in *Proceedings of the Pacific Rim Congress '90, 3*, 63-70, Australasian Institute of Mining Metallurgy, Parkville, Vic., 1990.

Weissel, J.K., and G.D. Karner, Flexural uplift of rift flanks due to mechanical unloading of the lithosphere during extension, *J. Geophys. Res., 94*, 13,919-13,950, 1989.

Wellman, P., Eastern Highlands of Australia: Their uplift and erosion, *BMR J. Aust. Geol. Geophys., 10*, 277-286, 1987.

White, R.S., and D.P. McKenzie, Magmatism at rift zones: The generation of volcanic continental margins and flood basalts, *J. Geophys. Res., 94*, 7685-7729, 1989.

Ziegler, P.A., Geodynamic processes governing development of rifted basins, in *Proc. Symposium Geodynamic Evolution of Sedimentary Basins*, edited by F. Roure et al., Editions Technip, Paris, in press, 1994.

P.A.M. Andriessen, S.A.P.L. Cloetingh, and P.A. van der Beek, Faculty of Earth Sciences, Vrije Universiteit, De Boelelaan 1085, 1081 HV Amsterdam, the Netherlands. (e-mail: beep@geo.vu.nl)

(Received February 18, 1994;
revised August 8, 1994;
accepted September 6, 1994.)